Inorganic Chemistry

Article

pubs.acs.org/IC

Single-Molecule-Magnet Behavior in a [2 × 2] Grid Dy^{III}_4 Cluster and a Dysprosium-Doped Y^{III}_4 Cluster

Peng-Hu Guo,[†] Jiang Liu,[†] Zi-Hao Wu, Hua Yan, Yan-Cong Chen, Jian-Hua Jia,* and Ming-Liang Tong*

MOE Key Lab of Bioinorganic and Synthetic Chemistry, School of Chemistry & Chemical Engineering, Sun Yat-Sen University, Guangzhou 510275, P. R. China

Supporting Information

ABSTRACT: Thanks to the MeCN hydrolysis in situ reaction, a [2 × 2] square grid Dy^{III}_4 cluster based on a polypyridyl triazolate ligand, $[Dy_4(OH)_2(bpt)_4(NO_3)_4(OAc)_2]$ (**1**), was separated successfully and characterized through single-crystal X-ray diffraction and SQUID magnetometry. The frequency-dependent signals in the out-of-phase component of the susceptibility associated with slow relaxation of the magnetization confirmed that complex **1** displays single-molecule magnet (SMM) behavior. Two distinct slow magnetic relaxation processes, with effective energy barriers U_{eff1} = 93 cm^{-1} for fast relaxation and U_{eff2} = 143 cm^{-1} for slow relaxation observed under a zero direct-current field, are mainly attributed to the origin of single-ion behavior, which can be further acknowledged by the magnetic investigation of a dysprosium-doped yttrium cluster. Besides, it should be noted that complex **1** represents so far the highest energy barrier among the pure Dy^{III}_4 SMMs.

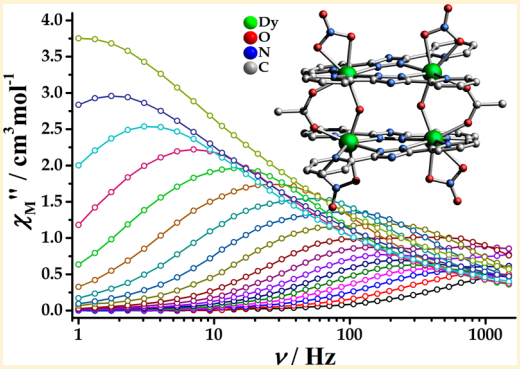

INTRODUCTION

Single-molecule magnets (SMMs) have been attracting much attention for their potential applications in ultrahigh-density information storage, molecular spintronics, and quantum information processing.[1] The key point leading to the SMM behavior arises from the large magnetic anisotropy, which gives rise to a significant energy barrier for the reversal of magnetization (U_{eff}).[2,3] In this context, it is preferred to explore lanthanide (Ln)-based systems in pursuit of SMMs with high U_{eff} because of the strong spin−orbit coupling commonly observed in Ln ions.[3n−p] For pure Ln-SMMs, the Dy^{III} ion may hold the key to obtaining higher U_{eff} because of its large magnetic anisotropy originating from the $^6H_{15/2}$ state.[4] In parallel, slow relaxation can be observed in Dy^{III}-only clusters with different core topologies, e.g., triangle,[3a,5a−c] defect-dicubane,[4a−d] linear,[6] grid,[7] square-pyramidal,[3c,8] wheel,[9] etc. Winpenny et al. have recorded the highest U_{eff} value, up to 367 cm^{-1} (528 K), for a Dy^{III}_5 SMM with a square-pyramidal topology.[3c]

In a quest for the magnetic behavior for Ln-based polynuclear species, we had decided to prepare a Dy^{III}-only compound involving a 3,5-bis(pyridin-2-yl)-1,2,4-trizole (Hbpt) ligand (Scheme 1). Recent achievements reveal our success in preparing a series of pure bpt-based Dy^{III} SMMs, namely, three Dy^{III}_4, one Dy^{III}_8, and one Dy^{III}_{10} with four types of topologies.[4c−f] The favorable U_{eff} values were found to lie from 31 to 81 cm^{-1} in the absence of an extra direct-current (dc) field. Among these bpt-based Dy^{III} SMMs, our attention has been paid to pure Dy^{III}_4 clusters with core topology such as butterfly[4c,d] and zigzag.[4e] In light of further analysis on the molecular structure and synthetic method, we draw a conclusion that Hbpt used in the preparation of SMMs plays the following roles: (i) two pockets for encapsulating the Ln centers, (ii) a rigid structure dictating the core arrangement, and (iii) a topology change by solvent molecules or linkers coordinated on vacant sites.

Scheme 1. Structure of the Hbpt Ligand

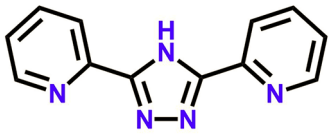

Hbpt

With these considerations in mind, we focused on the preparation of pure Dy^{III}_4 clusters with distinct topology and higher U_{eff} as an extension of our previous bpt-based studies. Herein we report a new Dy^{III}_4 cluster, $[Dy_4(OH)_2(bpt)_4(NO_3)_4(OAc)_2]$ (Dy_4, **1**). By the self-assembly of Hbpt and $Dy(NO_3)_3{\cdot}6H_2O$ under MeCN solvothermal conditions, blocklike colorless crystals of **1** have been separated successfully. Interestingly, different from what was reported previously by our group, the Dy^{III}_4 core topology in **1** belongs to neither the butterfly nor the zigzag arrangement; instead, it is a kind of square grid. Moreover, a record value for **1**, U_{eff} = 143 cm^{-1} (206 K), is found among all

Received: June 11, 2015
Published: August 6, 2015

DOI: 10.1021/acs.inorgchem.5b01322
Inorg. Chem. 2015, 54, 8087−8092

pure Dy^{III}_4 SMMs. Additionally, to verify the origin of slow magnetic relaxation of **1**, a dysprosium-doped yttrium cluster, $[Dy_{0.24}Y_{3.76}(OH)_2(bpt)_4(NO_3)_4(OAc)_2]$ (Dy@Y_4, **2**), has been synthesized and characterized magnetically. Magnetic studies indicate that the two relaxation processes that appeared may originate from the single-ion behavior of the individual dysprosium ion within the cluster.

EXPERIMENTAL SECTION

Materials and General Procedures. All of the reagents employed were commercially available and were used as received without further purification. Magnetic susceptibility measurements were performed on a Quantum Design PPMS instrument. All alternating-current (ac) susceptibility data from 1 to 1488 Hz were collected under a zero dc field. The sample was packed into the cling film, which was then mounted in low-background diamagnetic plastic straws. The data were corrected for the magnetization of the sample holder and the diamagnetism of the constituent atoms using Pascal constants. C, H, and N microanalyses were performed on a fresh sample, which was taken out immediately from the mother liquor, with an Elementar Vario-EL CHN elemental analyzer. Fourier transform infrared spectra were recorded in KBr tablets in the range 4000−400 cm^{-1} on a Bio-Rad FTS-7 spectrometer. Powder X-ray diffraction (PXRD) intensities were measured at 293 K on a Bruker D8 Advance diffractometer (Cu Kα, λ = 1.54056 Å) by scanning over the range of 5−50° with steps of 0.2°/s. An accurate yttrium/dysprosium ratio was measured using the inductively coupled plasma (ICP) atomic emission spectra analyzed by a TJA IRIS(HR) spectrometry.

*$[Dy_4(OH)_2(bpt)_4(NO_3)_4(OAc)_2]$ (Dy_4, **1**).* Hbpt (0.1 mmol, 0.023 g) and MeCN (8 mL) were added to a 23 mL Teflon-lined reactor and then dissolved by an ultrasonic bath for 10 min at room temperature. Then $Dy(NO_3)_3·6H_2O$ (0.1 mmol, 0.045 g) was added, and the subsequent solution was heated at 160 °C for 72 h followed by cooling to room temperature at a rate of 5 °C/h. Colorless blocklike crystals along with white amorphous powder were obtained. The products were washed with analytically pure MeCN three times and collected by filtration. The pure colorless crystals were manually separated under a microscope. Yield: 34% of pure crystals (based on Dy). The purity of the bulk samples was confirmed by a comparison of the experimental PXRD pattern with that calculated from the single-crystal study (Figure S1). Elem anal. Calcd for $C_{52}H_{40}N_{24}O_{18}Dy_4$: C, 32.21; H, 2.08; N, 17.34. Found: C, 32.06; H, 2.20; N, 17.10.

*$[Dy_{0.24}Y_{3.76}(OH)_2(bpt)_4(NO_3)_4(OAc)_2]$ (Dy@Y_4, **2**).* . The magnetically dilute sample, Dy@Y_4, was obtained by combining accurately measured amounts of $Dy(NO_3)_3·6H_2O$ and $Y(NO_3)_3·6H_2O$ in a 1:19 molar ratio, following the procedure described above. It should be noted that, however, the resulting doped ratio is 1:16, a non-stoichiometric product, even a reaction with an accurate starting ratio. The purity of the bulk samples was confirmed by a comparison of the experimental PXRD pattern with that calculated from the single-crystal study (Figure S1). Elem anal. Calcd for $C_{52}H_{40}N_{24}O_{18}Dy_{0.24}Y_{3.76}$: C, 37.47; H, 2.42; N, 20.17. Found: C, 37.57; H, 2.43; N, 20.22. The amount of Dy^{III} in **2** (6%) is confirmed by the ICP measurement.

X-ray Crystallography. Diffraction intensities of **1** and **2** were collected at 298(2) K on a Rigaku R-AXIS SPIDE image-plate diffractometer with Mo Kα radiation. The structures were solved by direct methods, and all non-hydrogen atoms were refined anisotropically by least squares on F^2 using the *SHELXTL* program.[10] Hydrogen atoms on organic ligands were generated by the riding mode. Crystal data and structural refinement are listed in Table 1. CCDC 1054224 (**1**; see the Supporting Information) and 1405886 (**2**; see the Supporting Information) contain the supplementary crystallographic data for this paper. These data can be obtained free of charge from The Cambridge Crystallographic Data Centre via www.ccdc.cam.ac.uk/data_request/cif [or fax (+44) 1223-336-033 or e-mail deposit@ccdc.cam.ac.uk].

Table 1. Crystal Data and Structural Refinement for 1 and 2

	1	2
empirical formula	$C_{52}H_{40}N_{24}O_{18}Dy_4$	$C_{52}H_{40}N_{24}O_{18}Dy_{0.24}Y_{3.76}$
fw	1939.08	1662.38
temperature/K	298(2)	298(2)
cryst syst	monoclinic	monoclinic
space group	$P2_1/n$	$P2_1/n$
a/Å	11.9694(4)	12.1909(5)
b/Å	17.0199(4)	16.8969(8)
c/Å	15.5030(5)	15.4868(6)
β/deg	92.784(1)	92.091(1)
V/Å^3	3154.51(16)	3188.2(2)
Z	2	2
ρ_{calc}/g cm^{-3}	2.041	1.732
μ/mm^{-1}	4.773	3.755
reflns collected	7121	7198
reflns unique	5419	5072
R(int)	0.0498	0.0581
GOF on F^2	1.108	1.018
R1[a] [$I > 2\sigma(I)$]	0.0428	0.0394
wR2[b] (all data)	0.1133	0.0942

[a] $R1 = \sum||F_o| - |F_c||/\sum|F_o|$. [b] $wR2 = [\sum w(F_o^2 - F_c^2)^2/\sum w(F_o^2)^2]^{1/2}$.

RESULTS AND DISCUSSION

Synthesis. Complex **1** was prepared successfully under solvothermal conditions from the reaction of $Dy(NO_3)_3·3H_2O$ and Hbpt in molar ratio of 1:1 in MeCN at 160 °C. Hydrolysis of MeCN led to in situ formation of the OAc^- group as a ligand. This is a common fact for C≡N^- moiety hydrolysis under high temperature. The OAc^- groups were confirmed and distinguished with NO_3^- units by IR spectrometry (Figure S2), as well as the bond distances of N−O and C−C shown in Figure S3. The elemental analysis data also support the point above. Upon integration with our previous work, three types of Dy^{III}_4 arrangement were found for the reaction of $Dy(NO_3)_3$ and Hbpt ligands, that is, butterfly (planar tetranuclear core),[4c,d] zigzag,[4e] and [2 × 2] square grid in this work. The key point to obtain various tetranuclear arrangements is control of the alkali and solvents in a reaction system. With the presence of Et_3N in the reactions, two types of butterfly-shaped Dy^{III}_4 cores were generated; on the contrary, the zigzag one formed. In parallel, once MeCN was used as the solvent instead of alcohols, a [2 × 2] grid of the Dy^{III}_4 core was observed, owing to hydrolysis of the C≡N^- moiety.

Crystal Structure. Complexes **1** and **2** are isostructural and crystallize in the monoclinic space group $P2_1/n$. The molecular structure of **1** is described as representative (Figure 1). Complex **1** features a tetranuclear arrangement of the Dy^{III}_4 core with crystallographic centrosymmetry. The four Dy^{III} ions, therefore, are strictly coplanar and form a [2 × 2] grid. The coordination geometries for Dy^{III} ions in a asymmetry unit were performed by continuous-shape measurements (CShM) using *SHAPE 2.0* software.[11] The calculated results listed in Table S1 reveal that both Dy1 and Dy2 possess triangular dodecahedral geometries with a N_4O_4 coordination environment (Figure S4).

Dy1 and Dy2 are chelated by two deprotonated μ-bpt^- ligands in the equatorial plane, resulting in a *trans*-$\{Dy_2(bpt)_2\}$ subunit (Figure 2). In contrast to the previous work, this is similar to the complex with a zigzag Dy^{III}_4 core[4e,12] but different from two butterfly cases with *cis*-$\{Dy_2(bpt)_2\}$ parts (Table 2).[4c,d] Two $\{Dy_2(bpt)_2\}$ subunits are further bridged by a pair of μ-OH^- and μ-OAc^- groups in a face-to-face fashion. Thus, a

DOI: 10.1021/acs.inorgchem.5b01322
Inorg. Chem. 2015, 54, 8087−8092

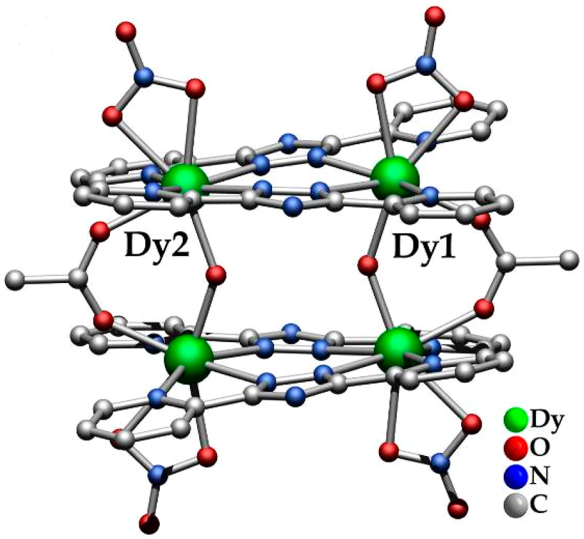

Figure 1. Molecular structure of **1**. Hydrogen atoms are omitted for clarity. Color code: Dy, green; O, red; N, blue; C, gray.

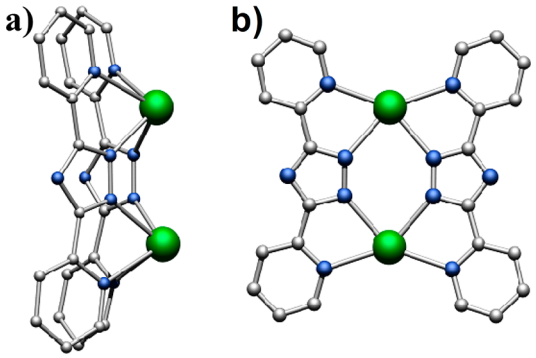

Figure 2. (a) *cis*- and (b) *trans*-$\{Dy_2(bpt)_2\}$ subunits.

Table 2. Relaxation Barrier for Selected Dy^{III}-Only SMMs with Different Tetranuclear Core Arrangements under a Zero dc Field

complex[a]	Dy^{III}_4 core arrangement	U_{eff}/cm^{-1} (K)	ref
$[Dy_4(OH)_2(bpt)_4(NO_3)_4(OAc)_2]$	square grid	143 (206)	this work
$[Dy_4(L1)_4(MeOH)_6]\cdot 2MeOH$	linear	120 (173)	6d
$Dy_4(OH)_2(bmh)_2(msh)_4Cl_2$	butterfly[b,c]	118 (170)	4a
$[Dy_4(OH)_2(bpt)_4(OMe)_2(NO_3)_4]\cdot 3MeOH$	butterfly[b]	81 (116)	4c
$[Dy_4\{H_3(L2)\}_2(OAc)_6]\cdot 2EtOH$	butterfly[b]	74 (107)	4b
$[Dy_4(L3)_2\{H(L3)\}_2(N_3)_4(O)]\cdot 14H_2O$	square grid	63 (91)	7a
$[Dy_4(OH)_4(bpt)_4(NO_3)_4(EtOH)_2]$	butterfly[b]	56 (80)	4d
$[Li(thf)_4][Dy_4\{N(SiMe_3)_2\}_4(SEt)_9]$	square grid	46 (66)	7d
$[Dy_4(OH)_2(bpt)_4(NO_3)_6(EtOH)_2]\cdot EtOH$	zigzag	31 (45)	4e
$[Dy_4(OH)_4(L4)_6(py)(MeOH)_7](ClO_4)_2\cdot py\cdot 4MeOH$	cubane	28 (40)	4g

[a] $H_3(L1)$ = [(2-hydroxy-3-methoxyphenyl)methylene] hydrazide; H_2bmh = 1,2-bis(2-hydroxy-3-methoxybenzylidene) hydrazine; Hmsh = 3-methoxysalicylaldehyde hydrazine; bpt = 3,5-bis(pyridin-2-yl)-1,2,4-trizaole; $H_6(L2)$ = 1,3-bis[tris(hydroxymethyl)-methylamino]propane; $H_2(L3)$ = bis(methyl 2-pyridyl ketone)-carbonohydrazone; thf = tetrahydrofuran; H(L4) = isonicotinic acid; py = pyridine. [b] Planar tetranuclear core. [c] Defect dicubane.

[2 × 2] square grid formed. The vacant coordination sites of each Dy^{III} ion are occupied by two NO_3^- groups. Selected bond lengths and angles are given in Table S2. The Dy−O and Dy−N bond lengths lie in the ranges of 2.211(5)−2.577(5) and 2.480(5)−2.559(6) Å, respectively. The Dy1−O−Dy2(A) bond angle bridged by μ-OH^- is 141.8(2)°. The intramolecular Dy1···Dy2 and Dy1···Dy2(A) distances are 5.062 and 4.183 Å, while the closest distance of the intermolecular $Dy^{III}\cdots Dy^{III}$ is 7.623 Å. Intramolecular hydrogen bonds are found with lengths of 2.873, 2.542, and 2.746 Å separately according with O1···H10, O2···H1, and O4···H1 (Figure S3). Until now, the examples of Dy^{III}_4 SMMs with a [2 × 2] grid are numbered,[7] and some of them have a μ_4-O^{2-} or μ_4-SEt bridge connecting four Dy^{III} centers.[7a−d]

Magnetic Properties. The magnetic susceptibilities of polycrystalline samples for **1** were measured using a SQUID magnetometer from 2 to 300 K at a 500 Oe dc field. The test results were plotted as $\chi_M T$ versus T, as shown in Figure 3a.

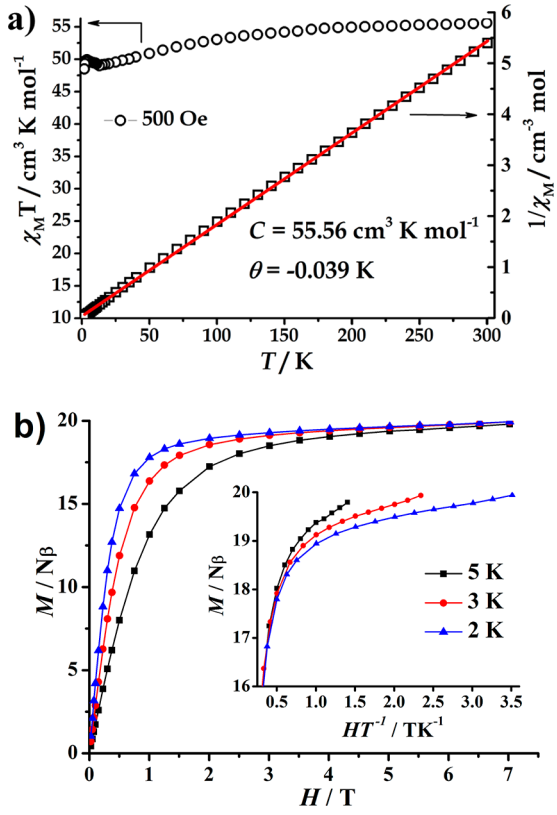

Figure 3. (a) $\chi_M T$ versus T and $1/\chi_M$ versus T plots for **1** with a Curie−Weiss fitting as the red line. (b) M versus H and the enlarged view of M versus HT^{-1} plots (inset) for **1**. Solid lines are guides for the eye.

The $\chi_M T$ value is approximately 55.60 cm^3 K mol^{-1} at 300 K, which is in agreement with the expected theoretical value of 56.7 cm^3 K·mol^{-1} for four noninteracting Dy^{III} ions ($^6H_{15/2}$, S = $^5/_2$, L = 5, g = $^4/_3$, C = 14 cm^3 K mol^{-1}).[13] The $\chi_M T$ value gradually decreases to 49.01 cm^3 K mol^{-1} at 13.00 K with decreasing temperature probably because of the thermal depopulation of the Stark levels for a single dysprosium ion, while a subsequent increase to a maximum of 49.92 cm^3 K mol^{-1} at 3.80 K may be attributed to the presence of weak ferromagnetic interactions between the spin carriers.[14] Upon further lowering of the temperature, the $\chi_M T$ value sharply

DOI: 10.1021/acs.inorgchem.5b01322
Inorg. Chem. 2015, 54, 8087−8092

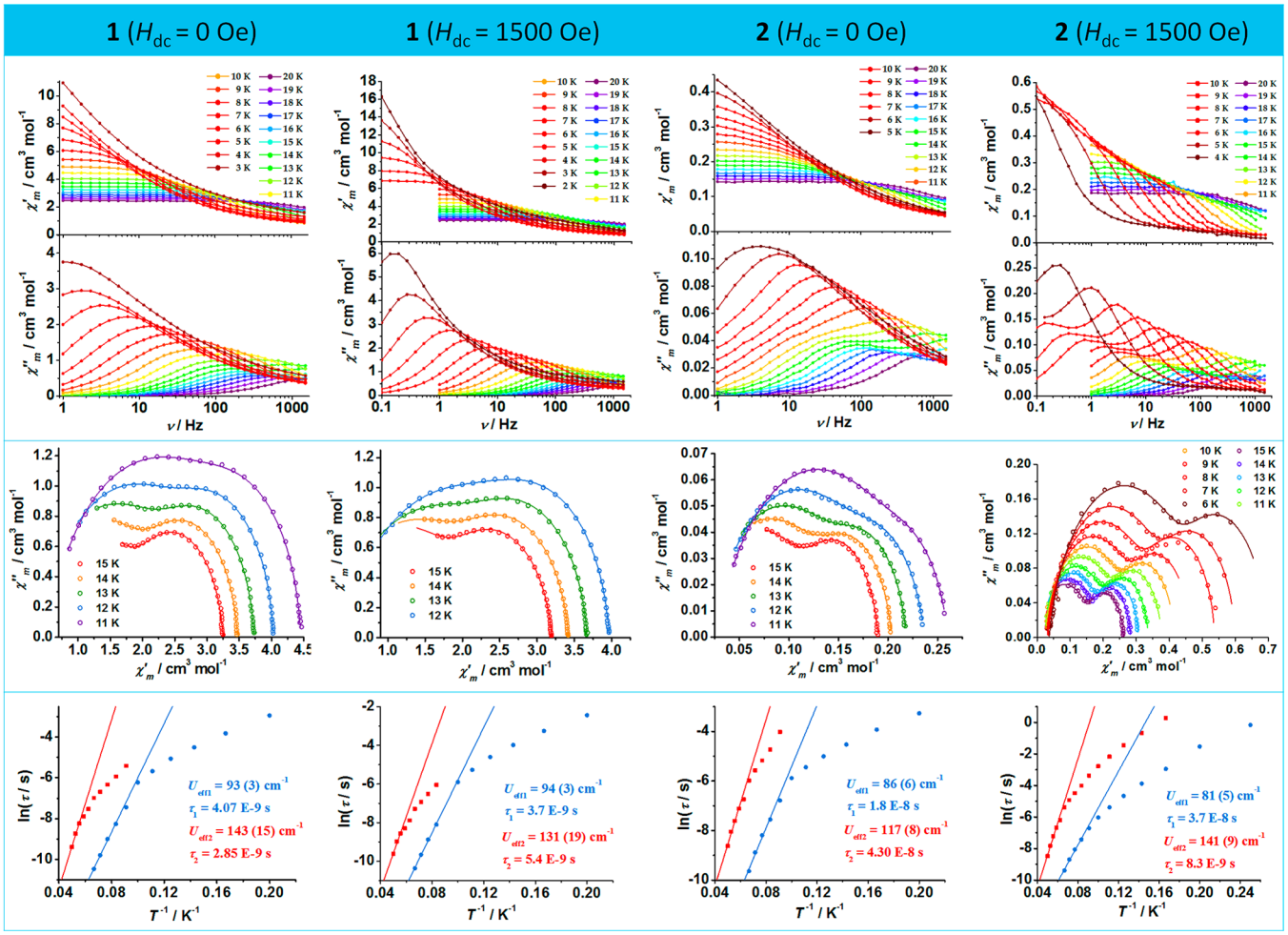

Figure 4. Plots of the frequency-dependent in-phase (χ_M') and out-of-phase (χ_M'') ac susceptibility at indicated temperatures (top), Cole−Cole diagrams with solid lines as Debye fits (middle), and magnetic relaxation time τ versus T^{-1} plots with linear fits of the thermally activated region (bottom) for **1** and **2**, respectively, under assigned fields.

decreases to a minimum of 48.49 cm^3 K mol^{-1}, which is likely ascribed to the presence of magnetic anisotropy and/or intermolecular weak antiferromagnetic interactions.[15] The fit of the experimental χ_M data to the Curie−Weiss law in the temperature range of 300−2 K results in the Curie constant (C = 55.56 cm^3 K mol^{-1}) and a very small Weiss temperature (θ = −0.039 K), suggesting very weak antiferromagnetic interactions overall.

The field dependence of magnetization at 2, 3, and 5 K shows that magnetization in the low H/T region becomes more rapidly saturated (Figure 3b), indicating the ferromagnetic interactions among four dysprosium ions. Furthermore, the nonsuperposition of the M versus H/T data on a single master curve means the presence of significant magnetic anisotropy in **1**.

ac magnetic susceptibility measurements were undertaken under a zero dc field between 3.0 and 20.0 K to further investigate the dynamic behavior of **1**. Both the in-phase (χ_M') and out-of-phase (χ_M'') plots (Figure 4) show frequency-dependent signals below 20.0 K. The broad peaks found in the out-of-phase ac susceptibility at 12.0 and 13.0 K indicate the presence of multiple slow relaxation processes. The temperature-dependent ac susceptibility plots are depicted in Figure 5. At high frequency, two separate peaks can be easily observed around 13 and 20 K in the out-of-phase ac susceptibility. This

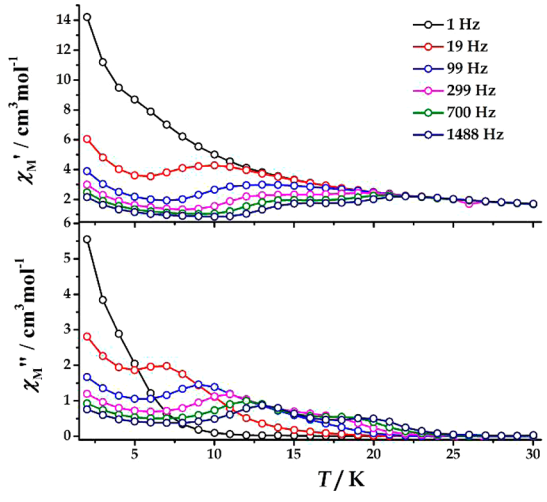

Figure 5. Temperature dependence of the in-phase (χ_M') and out-of-phase (χ_M'') ac susceptibility under H_{dc} = 0 Oe for **1**.

scenario indicates that there are two regimes of relaxation probably coming from two crystallographic dysprosium ions within **1**. It is not unfamilar for the Dy^{III}_4 grid decribed in the literature.[7] At the temperature region below 5 K, an increase of the ac reponse is commonly observed in the Ln SMMs and

DOI: 10.1021/acs.inorgchem.5b01322
Inorg. Chem. 2015, 54, 8087−8092

ascribed to the prevalent quantum tunneling of magnetization (QTM).[4] The field dependence of the relaxation rate for **1** reveals suppression of the QTM process upon application of the field because of the increase of the relaxation time observed in lower fields and then the decrease in higher fields with a peak maxmium of 1500 Oe (Figure S5).

The Cole−Cole plots in the form of χ_M' versus χ_M'' are shown in Figure 4. With an increase of the temperature, the fast relaxation (FR) and slow relaxation (SR) gradually separate and coexist between 11 and 15 K. Upon a further increase of the temperature, FR diminishes after 16 K and SR dominates between 16 and 20 K (Figure S6).

The relaxation time was extracted by fitting the Cole−Cole plots between 3 and 20 K (Figure S6). The frequency-dependent ac susceptibility data between 11 and 15 K can be successfully fitted to the modified two-step Debye model function, giving distribution coefficient values of 0.22−0.01 for both FR and SR,[16] which indicates the relatively moderate distribution of each relaxation time (Table S3). The data from 3 to 10 K are fitted to the generalized model, yielding α values of 0.28−0.59. This also indicates the occurrence of multiple relaxation mechanisms.[4a,17]

Plotting the relaxation time τ versus the temperature T^{-1} and a linear fitting of the thermally activated points to the Arrhenius law afford $U_{eff1} = 93(3)$ cm^{-1} and $\tau_1 = 4.07 \times 10^{-9}$ s for FR and $U_{eff2} = 143(15)$ cm^{-1} and $\tau_2 = 2.85 \times 10^{-9}$ s for SR (Figure 4). As far as we know, the latter is the highest energy barrier among the pure Dy^{III}_4 SMMs under a zero dc field (Table 2).[4−7] Under an optimum field of 1500 Oe, the frequency-dependent in-phase and out-of-phase ac susceptibility and magnetic relaxation time τ versus T^{-1} plots are shown in Figure 4. The resulting effective energy barrier and relaxation time are nearly identical with the values extracted from that under zero field.

To gain more insight into the origin of two relaxation processes for **1**, dynamic analysis of the doped species ($Dy@Y_4$, **2**) has been performed. ac measurements on **2** reveal that there is no obvious difference in the magnetic performance presented by **1** (Figure 4, top). Two slow magnetic relaxations, similarly, were again observed from the frequency-dependent ac susceptibilities, which can be further supported by the Cole−Cole plot showing the superposition of two semicircles at the fixed temperature area between 11 and 15 K (Figure 4, middle). The fitting of the Cole−Cole plot using a linear combination of two modified Debye functions generates α values ranging from 0.09 to 0.28, implying analogous distribution of the relaxation times (Table S4) with compound **1**. Accordingly, the two relaxation regimes can be mainly associated with the single-ion behavior of an individual dysprosium ion. Treating the data extracted from the Cole−Cole plot above 5 K with the Arrhenius model gives $U_{eff1} = 86(6)$ cm^{-1} and $\tau_1 = 1.8 \times 10^{-8}$ s for FR and $U_{eff2} = 117(8)$ cm^{-1} and $\tau_2 = 4.3 \times 10^{-8}$ s for SR (Figure 4, bottom). The resulting deviation of the effective energy barriers and relaxation times for complexes **1** and **2** is probably induced by subtle modification of the coordination geometries[18] around the dysprosium ions in a doped system. These structural differences are present as varied bond lengths and bond angles around dysprosium ions (Table S2). Of course, weak intramolecular ferromagnetic exchange could also play a role, which has already been demonstrated in most SMMs reported.[1e,3j] For **2**, the exchange coupling between the dysprosium ions virtually vanishes after dilution. The lower temperature data are markedly nonlinear, suggesting the onset of competition with other relaxation processes.

CONCLUSIONS

In this study, with the help of MeCN hydrolysis in situ, a [2 × 2] square-grid-shaped tetranuclear Dy^{III}_4 cluster showing SMM behavior with a remarkably high energy barrier (143 cm^{-1}) has been obtained under solvothermal conditions. A further magnetic investigation of the dysprosium-doped yttrium cluster reveals that two distinct slow magnetic relaxation processes are mainly attributed to the origin of single-ion behavior. The discovery above not only significantly improves the magnetic property of the bpt$^-$-bridged complexes but also holds the hightest U_{eff} value among the pure Dy^{III}_4 SMMs. Modification of the Hbpt ligand and introduction into auxiliary groups will be undergoing next to systematically modulate the local symmetry of Dy^{III} ions to further enhance the magnetic properties.

ASSOCIATED CONTENT

Supporting Information

The Supporting Information is available free of charge on the ACS Publications website at DOI: 10.1021/acs.inorgchem.5b01322.

IR spectrum, PXRD patterns, selected bond lengths and angles, and figures of magnetic characterization (PDF)
Crystallographic data in CIF format for **1** (CIF)
Crystallographic data in CIF format for **2** (CIF)

AUTHOR INFORMATION

Corresponding Authors

*E-mail: jiajh3@mail.sysu.edu.cn.
*E-mail: tongml@mail.sysu.edu.cn..

Author Contributions

†These authors contributed equally to this work.

Notes

The authors declare no competing financial interest.

ACKNOWLEDGMENTS

This work was supported by the "973 Project" (Grants 2014CB845602 and 2012CB821704), the NSFC (Grants 91122032, 91422302, 21301197, and 21371183), the NSF of Guangdong (Grant S2013020013002), the Program for Changjiang Scholars and Innovative Research Team in University of China, and the Fundamental Research Funds for the Central Universities (14lgpy10).

REFERENCES

(1) (a) Leuenberger, M. N.; Loss, D. *Nature* **2001**, *410*, 789−793. (b) Miller, J. S.; Gatteschi, D. *Chem. Soc. Rev.* **2011**, *40*, 3065−3066. (c) Aromí, G.; Aguilà, D.; Gamez, P.; Luis, F.; Roubeau, O. *Chem. Soc. Rev.* **2012**, *41*, 537−546. (d) Clemente-juan, J. M.; Coronado, E.; Gaita-Ariño, A. *Chem. Soc. Rev.* **2012**, *41*, 7464−7478. (e) Woodruff, D. N.; Winpenny, R. E. P.; Layfield, R. A. *Chem. Rev.* **2013**, *113*, 5110. (f) Mannini, M.; Pineider, F.; Danieli, C.; Totti, F.; Sorace, L.; Sainctavit, Ph.; Arrio, M.-A.; Otero, E.; Joly, L.; Cezar, J. C.; Cornia, A. A.; Sessoli, R. *Nature* **2010**, *468*, 417−421. (g) Sessoli, R.; Boulon, M.-E.; Caneschi, A.; Mannini, M.; Poggini, L.; Wilhelm, F.; Rogalev, A. *Nat. Phys.* **2014**, *11*, 69−74. (h) Mannini, M.; Pineider, F.; Sainctavit, P.; Danieli, C.; Otero, E.; Sciancalepore, C.; Talarico, A. M.; Arrio, M.-A.; Cornia, A.; Gatteschi, D.; Sessoli, R. *Nat. Mater.* **2009**, *8*, 194−197. (2) (a) Sessoli, R.; Gatteschi, D.; Caneschi, A.; Novak, M. A. *Nature* **1993**, *365*, 141−143. (b) Sessoli, R.; Tsai, H. L.; Schake, A. R.; Wang, S.; Vincent, J. B.; Folting, K.; Gatteschi, D.; Christou, G.; Hendrickson, D. N. *J. Am. Chem. Soc.* **1993**, *115*, 1804−1816. (c) Gatteschi, D.; Sessoli, R. *Angew. Chem., Int. Ed.* **2003**, *42*, 268−297. (d) Christou, G.;

DOI: 10.1021/acs.inorgchem.5b01322
Inorg. Chem. 2015, 54, 8087−8092

Gatteschi, D.; Hendrickson, D. N.; Sessoli, R. *MRS Bull.* **2000**, *25*, 66−71. (e) Wang, W.-G.; Zhou, A.-J.; Zhang, W.-X.; Tong, M.-L.; Chen, X.-M.; Nakano, M.; Beedle, C. C.; Hendrickson, D. N. *J. Am. Chem. Soc.* **2007**, *129*, 1014−1015. (f) Liu, J.-L.; Guo, F.-S.; Meng, Z.-S.; Zheng, Y.-Z.; Leng, J.-D.; Tong, M.-L.; Ungur, L.; Chibotaru, L. F.; Heroux, K. J.; Hendrickson, D. N. *Chem. Sci.* **2011**, *2*, 1268−1272.

(3) (a) Ishikawa, N.; Sugita, M.; Ishikawa, T.; Koshihara, S.; kaizu, Y. *J. Am. Chem. Soc.* **2003**, *125*, 8694−8695. (b) Hewitt, I. J.; Tang, J.; Madhu, N. T.; Anson, C. E.; Lan, Y.; Luzon, J.; Etienne, M.; Sessoli, R.; Powell, A. K. *Angew. Chem., Int. Ed.* **2010**, *49*, 6352−6356. (c) Blagg, R. J.; Ungur, L.; Tuna, F.; Speak, J.; Comar, P.; Collison, D.; Wernsdorfer, W.; McInnes, E. J. L.; Chibotaru, L. F.; Winpenny, R. E. P. *Nat. Chem.* **2013**, *5*, 673−678. (d) Tuna, F.; Smith, C. A.; Bodensteiner, M.; Ungur, L.; Chibotaru, L. F.; McInnes, E. J. L.; Winpenny, R. E. P.; Collison, D.; Layfield, R. A. *Angew. Chem., Int. Ed.* **2012**, *51*, 6976−6980. (e) Jiang, S. D.; Wang, B. W.; Sun, H. L.; Wang, Z. M.; Gao, S. *J. Am. Chem. Soc.* **2011**, *133*, 4730−4733. (f) Suzuki, K.; Sato, R.; Mizuno, N. *Chem. Sci.* **2013**, *4*, 596−600. (g) Rinehart, J. D.; Fang, M.; Evans, W. J.; Long, J. R. *Nat. Chem.* **2011**, *3*, 538−542. (h) Le Roy, J. J.; Ungur, L.; Korobkov, I.; Chibotaru, L. F.; Murugesu, M. *J. Am. Chem. Soc.* **2014**, *136*, 8003−8010. (i) Chen, L.; Wang, J.; Wei, J.-M.; Wernsdorfer, W.; Chen, X.-T.; Zhang, Y.-Q.; Song, Y.; Xue, Z.-L. *J. Am. Chem. Soc.* **2014**, *136*, 12213−12216. (j) Liu, J.-L.; Wu, J.-Y.; Chen, Y.-C.; Mereacre, V.; Powell, A. K.; Ungur, L.; Chibotaru, L. F.; Chen, X.-M.; Tong, M.-L. *Angew. Chem., Int. Ed.* **2014**, *53*, 12966−12970. (k) Ungur, L.; Le Roy, J. J.; Korobkov, I.; Murugesu, M.; Chibotaru, L. F. *Angew. Chem., Int. Ed.* **2014**, *53*, 4413−4417. (l) Jiang, S.-D.; Wang, B.-W.; Su, G.; Wang, Z.-M.; Gao, S. *Angew. Chem., Int. Ed.* **2010**, *49*, 7448−7451. (m) Rinehart, J. D.; Fang, M.; Evans, W. J.; Long, J. R. *J. Am. Chem. Soc.* **2011**, *133*, 14236−14239. (n) Cucinotta, G.; Perfetti, M.; Luzon, J.; Etienne, M.; Car, P.-E.; Caneschi, A.; Calvez, G.; Bernot, K.; Sessoli, R. *Angew. Chem., Int. Ed.* **2012**, *51*, 1606−1610. (o) Boulon, M.-E.; Cucinotta, G.; Luzon, J.; Degl'Innocenti, C.; Perfetti, M.; Bernot, K.; Calvez, G.; Caneschi, A.; Sessoli, R. *Angew. Chem., Int. Ed.* **2013**, *52*, 350−354. (p) Sessoli, R.; Powell, A. K. *Coord. Chem. Rev.* **2009**, *253*, 2328−2341.

(4) (a) Lin, P.-H.; Burchell, T. J.; Ungur, L.; Chibotaru, L. F.; Wernsdorfer, W.; Murugesu, M. *Angew. Chem., Int. Ed.* **2009**, *48*, 9489−9492. (b) Liu, C.-M.; Zhang, D.-Q.; Zhu, D.-B. *Dalton. Trans.* **2013**, *42*, 14813−14818. (c) Guo, P.-H.; Liu, J.-L.; Jia, J.-H.; Wang, J.; Guo, F.-S.; Chen, Y.-C.; Lin, W.-Q.; Leng, J.-D.; Bao, D.-H.; Zhang, X.-D.; Luo, J.-H.; Tong, M.-L. *Chem. - Eur. J.* **2013**, *19*, 8769−8773. (d) Guo, P.-H.; Liu, J.-L.; Zhang, Z.-M.; Ungur, L.; Chibotaru, L. F.; Leng, J.-D.; Guo, F.-S.; Tong, M.-L. *Inorg. Chem.* **2012**, *51*, 1233−1235. (e) Guo, P.-H.; Meng, Y.; Chen, Y.-C.; Li, Q.-W.; Wang, B.-Y.; Leng, J.-D.; Bao, D.-H.; Jia, J.-H.; Tong, M.-L. *J. Mater. Chem. C* **2014**, *2*, 8858−8864. (f) Guo, P.-H.; Liao, X.-F.; Leng, J.-D.; Tong, M.-L. *Acta Chim. Sin.* **2013**, *71*, 173−178. (g) Gao, Y.-J.; Xu, G.-F.; Zhao, L.; Tang, J.-K.; Liu, Z.-L. *Inorg. Chem.* **2009**, *48*, 11495−11497. (h) Das, S.; Dey, A.; Biswas, S.; Colacio, E.; Chandrasekhar, V. *Inorg. Chem.* **2014**, *53*, 3417−3426. (i) Alexandropoulos, D. I.; Cunha-Silva, L.; Pham, L.; Bekiari, V.; Christou, G.; Stamatatos, T. C. *Inorg. Chem.* **2014**, *53*, 3220−3229. (j) Xue, S.; Guo, Y.-N.; Zhao, L.; Zhang, P.; Tang, J. *Dalton. Trans.* **2014**, *43*, 1564−1570. (k) Sun, W.-B.; Han, B.-L.; Lin, P.-H.; Li, H.-F.; Chen, P.; Tian, Y.-M.; Murugesu, M.; Yan, P.-F. *Dalton. Trans.* **2013**, *42*, 13397−13403. (l) Yadav, M.; Mereacre, V.; Lebedkin, S.; Kappes, M. M.; Powell, A. K.; Roesky, P. W. *Inorg. Chem.* **2015**, *54*, 773−781. (m) Guo, F.-S.; Liu, J.-L.; Leng, J.-D.; Meng, Z.-S.; Lin, Z.-J.; Tong, M.-L.; Gao, S.; Ungur, L.; Chibotaru, L. F. *Chem. - Eur. J.* **2011**, *17*, 2458−2466.

(5) (a) Tang, J.; Hewitt, I.; Madhu, N. T.; Chastanet, G.; Wernsdorfer, W.; Anson, C. E.; Benelli, C.; Sessoli, R.; Powell, A. K. *Angew. Chem., Int. Ed.* **2006**, *45*, 1729−1733. (b) Lin, S.-Y.; Wernsdorfer, W.; Ungur, L.; Powell, A. K.; Guo, Y.-N.; Tang, J.; Zhao, L.; Chibotaru, L. F.; Zhang, H.-J. *Angew. Chem., Int. Ed.* **2012**, *51*, 12767−12771. (c) Xue, S.; Zhao, L.; Guo, Y.-N.; Zhang, P.; Tang, J. *Chem. Commun.* **2012**, *48*, 8946−898.

(6) (a) Guo, Y.-N.; Xu, G.-F.; Wernsdorfer, W.; Ungur, L.; Guo, Y.; Tang, J.; Zhang, H.-J.; Chibotaru, L. F.; Powell, A. K. *J. Am. Chem. Soc.* **2011**, *133*, 11948−11951. (b) Xu, G.-F.; Wang, Q.-L.; Gamez, P.; Ma, Y.; Clérac, R.; Tang, J.; Yan, S.-P.; Cheng, P.; Liao, D.-Z. *Chem. Commun.* **2010**, *46*, 1506−1508. (c) Lin, S.-Y.; Zhao, L.; Ke, H.; Guo, Y.-N.; Tang, J.; Guo, Y.; Dou, J. *Dalton Trans.* **2012**, *41*, 3248−3252. (d) Guo, Y.-N; Xu, G.-F; Gamez, P.; Zhao, L.; Lin, S.-Y; Deng, R.; Tang, J.; Zhang, H.-J. *J. Am. Chem. Soc.* **2010**, *132*, 8538−8539.

(7) (a) Anwar, M. U.; Thompson, L. K.; Dawe, L. N.; Habib, F.; Murugesu, M. *Chem. Commun.* **2012**, *48*, 4576−4578. (b) Xue, S.; Zhao, L.; Guo, Y.-N.; Chen, X.-H.; Tang, J. *Chem. Commun.* **2012**, *48*, 7031−7033. (c) Randell, N. M.; Anwar, M. U.; Drover, M. W.; Dawe, L. N.; Thompson, L. K. *Inorg. Chem.* **2013**, *52*, 6731−6742. (d) Woodruff, D. N.; Tuna, F.; Bodensteiner, M.; Winpenny, R. E. P.; Layfield, R. A. *Organometallics* **2013**, *32*, 1224−1229. (e) Xue, S.; Zhao, L.; Guo, Y.-N.; Tang, J. *Dalton Trans.* **2012**, *41*, 351−353. (f) Wu, S.-Q.; Xie, Q.-W.; An, G.-Y.; Chen, X.; Liu, C.-M.; Cui, A.-L; Kou, H.-Z. *Dalton Trans.* **2013**, *42*, 4369−4372.

(8) Gamer, M. T.; Lan, Y.; Roesky, P. W.; Powell, A. K.; Clérac, R. *Inorg. Chem.* **2008**, *47*, 6581−6583.

(9) (a) Westin, L. G.; Kritikos, M.; Caneschi, A. *Chem. Commun.* **2003**, 1012−1013. (b) Langley, S. K.; Moubaraki, B.; Forsyth, C. M.; Gass, I. A.; Murray, K. S. *Dalton Trans.* **2010**, *39*, 1705−1708. (c) Zhao, L.; Xue, S.; Tang, J. *Inorg. Chem.* **2012**, *51*, 5994−5996.

(10) Sheldrick, G. M. *Acta Crystallogr., Sect. A: Found. Crystallogr.* **2008**, *64*, 112−122.

(11) Li, Q.-W.; Liu, J.-L.; Jia, J.-H.; Leng, J.-D.; Lin, W.-Q.; Chen, Y.-C.; Tong, M.-L. *Dalton Trans.* **2013**, *42*, 11262−11270.

(12) Yang, P.-P.; Gao, X.-F.; Song, H.-B.; Zhang, S.; Mei, X.-L.; Li, L.-C.; Liao, D.-Z. *Inorg. Chem.* **2011**, *50*, 720−722.

(13) (a) Kahn, O. *Molecular Magnetism*; VCH Publishers: New York, 1993. (b) Benelli, C.; Gatteschi, D. *Chem. Rev.* **2002**, *102*, 2369−2388. (c) Sutter, J.-P.; Kahn, M. L. *Magnetism: molecules to materials*; Miller, J. S., Drillon, M., Eds.; Wiley-VCH: Weinheim, Germany, 2005; Vol. *5*, p 161.

(14) (a) Lin, P.-H.; Burchell, T.; Clérac, R.; Murugesu, M. *Angew. Chem., Int. Ed.* **2008**, *47*, 8848−8851. (b) Zheng, Y.-Z.; Evangelisti, M.; Tuna, F.; Winpenny, R. E. P. *J. Am. Chem. Soc.* **2012**, *134*, 1057−1065.

(15) Rinehart, J. D.; Long, J. R. *Chem. Sci.* **2011**, *2*, 2078−2085.

(16) (a) Grahl, M.; Kotzler, J.; Sessler, I. *J. Magn. Magn. Mater.* **1990**, *90-91*, 187−188. (b) Cole, K. S.; Cole, R. H. *J. Chem. Phys.* **1941**, *9*, 341−351.

(17) (a) Bi, Y.; Wang, X.-T.; Liao, W.; Wang, X.; Deng, R.; Zhang, H.; Gao, S. *Inorg. Chem.* **2009**, *48*, 11743−11747. (b) Yan, P.-F.; Lin, P.-H.; Habib, F.; Aharen, T.; Murugesu, M.; Deng, Z.-P.; Li, G.-M.; Sun, W.-B. *Inorg. Chem.* **2011**, *50*, 7059−7065.

(18) (a) Habib, F.; Long, J.; Lin, P.-H.; Korobkov, I.; Ungur, L.; Wernsdorfer, W.; Chibotaru, L. F.; Murugesu, M. *Chem. Sci.* **2012**, *3*, 2158−2164. (b) Li, Q.-W.; Liu, J.-L.; Jia, J.-H.; Chen, Y.-C.; Liu, J.; Wang, L.-F.; Tong, M.-L. *Chem. Commun.* **2015**, *51*, 10291−10294.

DOI: 10.1021/acs.inorgchem.5b01322
Inorg. Chem. 2015, 54, 8087−8092